Journal of Colloid and Interface Science 425 (2014) 91–95

Contents lists available at ScienceDirect

Journal of Colloid and Interface Science

www.elsevier.com/locate/jcis

New method for the simultaneous determination of diffusion and adsorption of dyes in silica hydrogels

Mercedes Perullini [a,*], Matías Jobbágy [a], María Laura Japas [b,c], Sara A. Bilmes [a,*]

[a] INQUIMAE-DQIAQF, Facultad de Ciencias Exactas y Naturales, Universidad de Buenos Aires, Ciudad Universitaria, Pab. II, C1428EHA Buenos Aires, Argentina
[b] Gerencia Química, Centro Atómico Constituyentes – CNEA, AV. Gral. Paz 1499, Pcia. de Buenos Aires, San Martín B1650KNA, Argentina
[c] ECyT, Universidad Nacional de San Martín, Argentina

ARTICLE INFO

Article history:
Received 11 January 2014
Accepted 13 March 2014
Available online 20 March 2014

Keywords:
Diffusion
Adsorption
Sol–gel
Silica hydrogel

ABSTRACT

The fine tuning of porosity in sol gel based devices makes possible the design of novel applications in which the transport of molecules through the oxide gel plays a crucial role. In this work we develop a new method for the simultaneous analysis of diffusion and adsorption of small diffusing probes, as anionic and cationic dyes, through silica mesoporous hydrogels synthesized by sol–gel. The novelty of the work resides in the simplicity of acquisition of the experimental data (by means of a desk scanner) and further mathematical modeling, which is in line with high throughput screening procedures, enabling rapid and simultaneous determination of relevant diffusion and adsorption parameters. Net mass transport and adsorption properties of the silica based hydrogels were contrasted to dye adsorption isotherms and textural characterization of the wet gels by SAXS, as well as that of the corresponding aerogels determined by Field Emission Scanning Electron Microscopy (FESEM) and N_2 adsorption. Thus, the validation of the results with well-established characterization methods demonstrates that our approach is robust enough to give reliable physicochemical information on these systems.

© 2014 Elsevier Inc. All rights reserved.

1. Introduction

Sol–gel processes provide a unique route for synthesizing inorganic materials at room temperature. By this route, novel materials have been obtained, such as mesoporous and nanostructured oxides, as well as a wide variety of hybrids [1,2]. The meso and microporous structures of sol–gel materials can be tuned by modifying the synthesis parameters, such as precursors, pH and additives, giving rise to oxide networks with well-defined porosity that are useful for the design of sensors, filtration devices or coatings [3,4].

The mild conditions of sol–gel routes are also appropriate for the design of novel bio-functional materials [5,6]. In particular, the encapsulation of different cell types including bacteria, yeasts, fungi and microalgae within silica hosts has become a well-established platform for enzymatic conversion, biosensing, and biomedical applications [7]. Several parameters can influence cell viability, such as gelation time [8], ionic strength [9] or cell/matrix interactions [10,11]. But, depending on their particular application, the optimization of viability must fulfill other needs, such as porosity, density, hardness and elasticity, which require a fine control of the synthesis parameters and a detailed characterization of their microstructure [12].

For any biological application, transport of molecules through the matrix results literally, of vital importance. In the first place, to fulfill nutrient diffusion required by actively growing cells [13,14], but also to allow the outcome of biosynthetic products of interest from encapsulation devices acting as modular bioreactors [15]. In several applications of these functional materials, such as remediation of contaminated water, transport of pollutants toward the encapsulated microorganisms must be controlled to regulate their concentration, in order to minimize harmful effects on the living species [16,17].

The transport within the water-filled regions in the space delineated by the silica skeleton can be fully described considering the size of the solute and the existence of charged groups on the skeleton which may bind the solute molecule will have an effect on the movement of the solute [18]. In the case of silica based hydrogels the polymer chain mobility can be neglected, as these hydrogels do not swell as it occurs with flexible polymeric hydrogels. Within a general approach, in mesoporous systems, mass transport involves at least two processes: diffusion and adsorption [19–21]. The last one is particularly important in silica hydrogels due to the high specific surface area, hydrophilicity and surface charge on pore walls (isoelectric point of silica ~pH 2) [22]. For almost

* Corresponding authors.
E-mail addresses: mercedesp@qi.fcen.uba.ar (M. Perullini), sarabil@qi.fcen.uba.ar (S.A. Bilmes).

http://dx.doi.org/10.1016/j.jcis.2014.03.030
0021-9797/© 2014 Elsevier Inc. All rights reserved.

all biomaterials based on silica, the working pH is near 7 and the surface charge plays an important role in the transport of positively charged molecules.

Many devices and methods have been developed to study solute transport in hydrogels; among them, fluorescence microscopy, isotope labeling, permeation, or electrochemical techniques are the most employed [23–25]. However, most of the published work does not present a full description of transport through these matrices since they discuss the diffusion in terms of pore size and tortuosity, not taking adsorption phenomena explicitly into account. On the other hand, several detailed mathematical models were proposed to account for diffusion–adsorption processes in porous media and polymer hydrogels [26–28]. Although these advanced tools and models are highly appropriate for the study the transport phenomena within silica matrices, simpler methods to obtain relevant parameters are needed in order to optimize the matrix transport properties when developing particular applications. In this scenario, the method proposed by Nakanishi et al. [29] (and its ensuing variants) was successfully used to measure diffusion and partition coefficients of several diffusing species in silica or silica-hybrid matrices [30,31]. Even these are relatively simple methods, the information concerning diffusion and adsorption phenomena is obtained in separate experiments.

The diffusion of colored moieties was used to calculate apparent diffusion coefficients, D_{app}, by digital image analysis of the concentration gradients at different elapsed times [32–34]. D_{app} is considered a parameter of practical relevance since it encompasses the retardation by adsorption and the tortuosity imposed by narrow pores, but it is only valid under restricted conditions. Parameters such as the concentration of free dye in solution as a function of distance and time elapsed cannot be derived from it.

In this work, we propose an extremely simple method based on digital image analysis for the simultaneous determination of dye diffusion and adsorption parameters on the silica hydrogel. The presented model, which considers diffusion coupled with adsorption occurring within the matrix, allows for the determination of an effective diffusion coefficient of the dye in the aqueous pores (D_{eff}).

Silica matrices were synthesized by silicate polymerization in the presence of LUDOX® silica nanoparticles. Varying the synthesis pH, the microstructure of silica hydrogels is modulated, and changes in the specific surface area and pore volume impact on the adsorption and diffusion processes, tuning the transport of dyes through these materials.

2. Materials and methods

2.1. Evaluation of transport properties

The protocol for monitoring the transport of dyes was based on the digital analysis of images [17]. In order to satisfy the boundary conditions for one-dimensional diffusion, the flow cell was made with two parallel glass slides (10.0 mm each side) separated by 1.0 mm layer of *in situ* prepared hydrogel. The dye is seeded on top of the hydrogel and the cell was placed on a digital scanner to acquire images of dye concentration profile at different times by sequential scanning. Color intensity profiles at each time are obtained by image analysis with ImageJ free software [35]. The values of color intensity are carefully restricted to the linear response range obtained with a proper calibration curve. To model the diffusion of Xylenol Orange (XO), as the anionic dye adsorption on negatively charged silica pores is found to be negligible, the effective diffusion coefficients were simply derived by fitting the concentration profiles to the second Fick equation:

$$\frac{\partial C}{\partial t} = D_{eff}\frac{\partial^2 C}{\partial^2 x} \tag{1}$$

The effective diffusion coefficient (D_{eff}) is defined as follows

$$D_{eff} = D\frac{\phi\delta}{\tau} \tag{2}$$

where D is the diffusion coefficient of the dye in water, ϕ is the pore volume fraction, δ is the constrictivity, and τ is the tortuosity of the matrix. The latter parameters allow describing the constraints imposed by mesopores to molecular free movement.

For a punctual source and assuming semi-infinite conditions (i.e., the dye does not reach the other side of the diffusing matrix throughout the whole time of the experiment), the diffusion profile is given by Eq. (4), where M is the initial amount of dye seeded:

$$C(x,t) = \frac{M}{\sqrt{\pi D_{eff} t}} e^{\frac{-x^2}{4D_{eff}t}} \tag{3}$$

To model the transport of the cationic dye Malachite Green (MG), where the process of diffusion is coupled with the adsorption on the silica surface, we represent the hydrogel as composed by N layers of thickness $dx = 10^{-3}$ cm (see Fig. S1 in Supplementary Information). The MG concentration in layer i at time j, $Q(i,j)$, is given by the sum of the concentration of dye in solution $C(i,j)$, and the dye adsorbed on silica surface, $S(i,j)$, at that time in the same layer. At time $t = 0$ all layers have a MG concentration $Q = 0$, except for the first layer at which the concentration equals to the total amount of dye seeded divided by the layer volume, $Q(1,0) = 6.00$ mM. The calculations were made using the Crank–Nicholson numerical method [36]. At each time step $dt = 3\ dx^2/D$, the partition between MG adsorbed and MG in solution is assumed to reach the adsorption equilibrium, and the diffusion of dye in solution is supposed to follow Fick first law. The parameters for fitting the experimental concentration profiles are D_{eff} (effective diffusion of the dye within the aqueous pores) and P that account for the partition of the dye between solution and silica surface.

2.2. Synthesis and supercritical drying of silica hydrogels

Silica sources are a sodium silicate solution (27 wt% SiO_2, 10 wt% NaOH from Riedel-de Haën) and colloidal silica (40 wt% SiO_2, LUDOX HS-40 from Aldrich). The aqueous synthesis of silica gels is performed as previously described [13]. Briefly, hydrochloric acid is added to a mixture containing sodium silicate and colloidal silica (LUDOX) in order to decrease the pH to the specified value. 1000 μL phosphate buffer and volumes of the different precursor solutions are adjusted to obtain a SiO_2:water molar relation of 3.8:100 with a proportion of polymeric to particulate silica precursors 1:4 in a final volume of 3.00 mL. In all cases the total silicon concentration is 2.1 M. In what follows, samples are labeled "HG-4.5", "HG-7" and "HG-9", for HydroGels synthesized at pH 4.5, 7.0 and 9.0, respectively. Except for syneresis experiments, for which samples are left in equilibrium with their mother liquors, hydrogel samples are washed thoroughly with distilled water 48 h after synthesis (at least 3 times of gelation), are then aged one week in phosphate buffer pH 6.5 and are washed thoroughly with distilled water prior to experiments.

Aerogels are prepared by supercritical CO_2 drying of hydrogels. Before drying, the samples are immersed in methanol for 2 days to reduce their water content; then they are transferred to a high-pressure quartz cell with fresh methanol. Supercritical CO_2 is passed through the cell at a flow rate of ca. 100 mL (NPT)/min while the pressure is kept constant at 9 MPa by a high-pressure syringe (Teledyne ISCO 100DM). Temperature is maintained at 55 °C during the whole procedure. The complete removal of methanol, realized by the absence of alcohol downstream, is achieved in

less than 3 h. The samples of aerogels are labeled AG-4.5, AG-7.0 and AG-9.0 (AeroGels derived from hydrogels synthesized at pH 4.5, 7.0 and 9.0, respectively).

2.3. Microstructure characterization of samples

Total volume of pores, ϕ_L, is obtained from the mass loss of the wet gels measured by thermal gravimetry (TG) carried out in a Shimadzu DTG50 thermal analyzer with a heating rate of 5 °C/min. Surface area and mesopore radii are determined from N_2 adsorption/desorption isotherms on the aerogels obtained from each hydrogel at 77 K on a Micromeritics 2010 sorptometer. Prior to each run the samples are degassed at 90 °C. Surface area is derived from the BET equation and pore radius from the capillary condensation in cylindrical pores using the classical Kelvin equation (BJH model) [37]. FESEM images of aerogels are taken with a Zeiss LEO 982 GEMINI microscope (CMA, FCEyN-UBA). Samples are metalized with gold for better image quality and stability.

2.4. Adsorption isotherms

For dye-adsorption experiments, samples of wet gels are left in contact with aliquots of 2000 μL of dye solution in different concentrations (aqueous solutions of MG or XO in the range 0.1–3.0 μM are adjusted to pH = 6.5). The concentration of dye in solution is measured spectrophotometrically at each dye absorbance maximum (λ = 616 nm for MG and λ = 436 nm for XO). The fraction of dye adsorbed on the silica matrix is calculated from the difference between the concentration in solution at t = 0 and after the systems had reach the equilibrium. For XO, under the experimental conditions adsorption is not significant. For the adsorption of MG, experimental data are fitted to the Freundlich model:

$$S = FC_e^n \tag{4}$$

where S is the mass of adsorbate by mass of adsorbent, F is the Freundlich constant of adsorption, C_e is the dye concentration in solution at equilibrium and n is a constant that varies from 0 to 1. This empirical model takes into account the heterogeneity of the different adsorption sites, being one of the most useful when analyzing adsorption from solution at the solid–liquid interface.

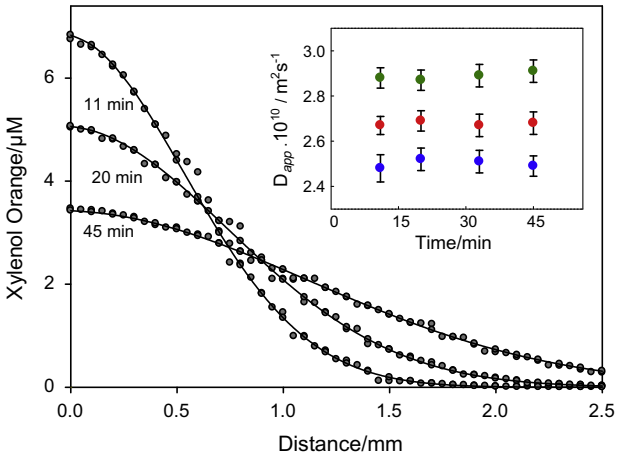

Fig. 1. Diffusional profiles of the anionic dye Xylenol Orange (XO) in silica hydrogel HG-4.5, taken at different sampling times: 11 min, 20 min and 45 min. The experimental XO concentration profiles can be fitted to the Fick's second law, describing a pure diffusive process. Inset: The apparent diffusion coefficients (D_{app}) obtained from each fitting as a function of sampling time for different hydrogel samples (HG-4.5: blue, HG-7.0: green and HG-9.0: red). (For interpretation of the references to color in this figure legend, the reader is referred to the web version of this article.)

3. Results and discussion

Evaluation of transport properties of the anionic dye Xylenol Orange (XO) and the cationic dye Malachite Green (MG) through the silica hydrogels is performed at pH 6.5, at which the silica surface is negatively charged (isoelectric point of silica ~pH 2). As stated above (Section 2.1), the physical system can be modeled as composed of multiple layers each of thickness dx, and a punctual source of the diffusing dye is seeded on an extended layer on top of the hydrogel. Since the gradient of concentration is established in the direction perpendicular to the thin layers, diffusion in one direction is assumed (see Fig. S1 in Supplementary Information).

The effective diffusion coefficient of the anionic dye XO derived by fitting the concentration profiles evaluated at different times to the second Fick equation is constant (Fig. 1). This indicates that for this dye we are dealing with a pure diffusive process, i.e. there is neither adsorption nor chemical reaction involved, and the apparent diffusion coefficient (D_{app}) equals the effective diffusion coefficient in the aqueous pores (D_{eff}). On the other hand, similar values of D_{app} (~D_{eff}) were obtained for the three hydrogels (Table 1).

The pore diameters derived from BJH model are at least one order of magnitude larger than the diffusing molecules (see Fig. S4 in Supplementary Information), thus giving little steric restriction to diffusion. Therefore, all samples should have similar tortuosity for diffusing species. Taking into account the pore fraction of each sample and disregarding tortuosity and constrictivity factors (see Eq. (2)), a unique XO diffusion coefficient $D_{XO} = (2.7 \pm 0.2)\ 10^{-10}$ m^2 s^{-1} was derived from all samples. This value is comparable to that obtained for a parent dye bromophenol blue in 1% agar gel ($D = (4.58 \pm 0.3)\ 10^{-10}$ m^2 s^{-1}) [38], as well as for diffusion of several charged species not adsorbed on silica. For instance, the

Table 1
Diffusion and adsorption parameters derived from the transport model and correlations to empirical results obtained in MG adsorption isotherms and specific adsorption areas and pore fraction volumes derived from aerogel porosimetry.

Sample	AG pore volume/cm^3 g^{-1}[a]	Pore volume fraction (ϕ)[b]	XO D_{eff}[c]/ 10^{-10} m^2 s^{-1}	MG D_{eff}[d]/ 10^{-10} m^2 s^{-1}	Parameter P [d]/10^3	Empirical Partition coeff. P_{emp}[e]/10^3	Specific sorption area (f [f]/10^6 cm^{-1}
HG-4.5/AG-4.5	0.60; 0.57	0.88 ± 0.01	2.5 ± 0.1	1.3 ± 0.1	6.1 ± 0.2	6.2 ± 0.6	11.3 ± 0.4
HG-7.0/AG-7.0	0.66; 0.65	0.92 ± 0.01	2.9 ± 0.1	1.4 ± 0.1	2.7 ± 0.1	3.8 ± 0.4	6.3 ± 0.3
HG-9.0 AG-9.0	0.53; 0.60	0.89 ± 0.01	2.7 ± 0.1	1.3 ± 0.1	3.3 ± 0.2	3.8 ± 0.4	7.7 ± 0.3

[a] From aerogel porosimetry (BJH Adsorption cumulative pore volume; BJH Desorption cumulative pore volume).
[b] From thermogravimetric analysis of hydrogels.
[c] Xylenol Orange effective diffusion coefficient obtained from the fitting of XO concentration profiles to Fick law describing a pure diffusive process.
[d] Malachite Green effective diffusion coefficient and values of parameter P obtained from the fitting of MG concentration profiles to the model of diffusion with adsorption described in Section 2.1.
[e] Empirical partition coefficient derived from MG adsorption isotherms (for an equilibrium concentration of 0.01 μM).
[f] Calculated from the from aerogel porosimetry (BET surface area = $a_{s,BET}$), the density of silica (theoretical value δ_{SiO2} = 2.65 g cm^{-3}) and the pore fraction volume (ϕ) as f (in cm^{-1}) = $a_{s,BET}$. δ_{SiO2}. $(1-\phi)$.

effective diffusion coefficient for Cr(IV) in silica hydrogels synthesized from colloidal silica is between 1.76 10^{-10} m^2 s^{-1} and 8.48 10^{-10} m^2 s^{-1}, depending on the silica content of the matrix [30]. For the diffusion of Ni^{2+} ion in TEOS derived silica matrices, a diffusion coefficient between 4.1 10^{-10} m^2 s^{-1} and 7.0 10^{-10} m^2 s^{-1} was determined for pore sizes bigger than 5 nm [39]. On the contrary, for matrices with pore sizes smaller than 5 nm, retarding factors from 10^2 to 10^3 were observed. It is worth noting that these systems have smaller mesopore sizes than the hydrogels prepared from colloidal silica and silicate at any pH value.

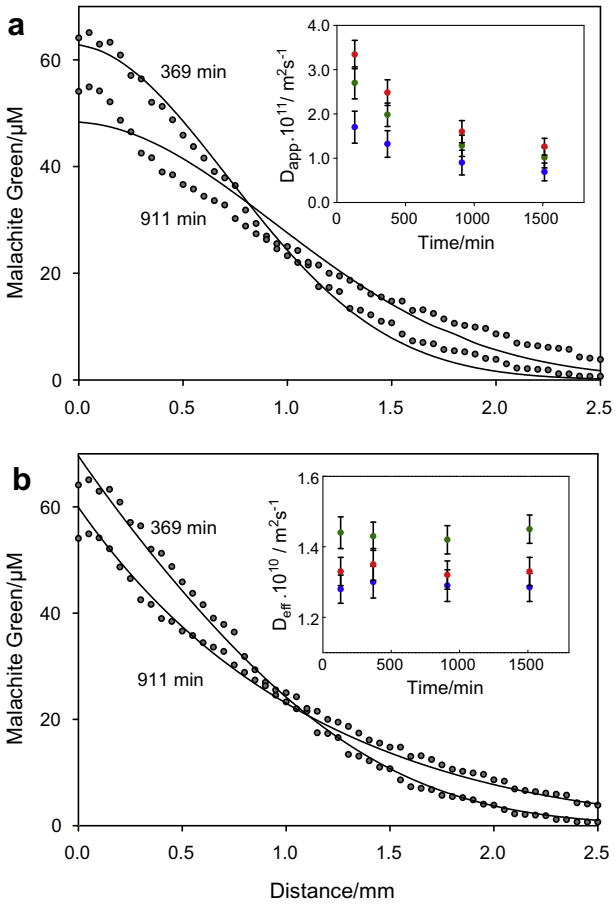

Fig. 2. Diffusional profiles of the cationic dye Malachite Green in silica hydrogel HG-4.5, taken at different sampling times: 369 min and 911 min. a: The experimental MG concentration profiles were fitted to the second Fick law, describing a pure diffusive process. Inset: The apparent diffusion coefficients (D_{app}) obtained from each fitting as a function of sampling time (from 130 to 1512 min) for different hydrogel samples (HG-4.5: blue, HG-7.0: green and HG-9.0: red). b: The experimental MG concentration profiles are fitted by a numerical method to the proposed model considering diffusion coupled with adsorption on the silica surface. Inset: The effective diffusion coefficients (D_{eff}) obtained from each fitting as a function of sampling time (from 130 to 1512 min) for different hydrogel samples (HG-4.5: blue, HG-7.0: green and HG-9.0: red). (For interpretation of the references to color in this figure legend, the reader is referred to the web version of this article.)

The diffusion of the cationic dye MG analyzed with the same protocol gives an apparent diffusion coefficient (D_{app}) that varies both in distance and in time. Fig. 2a shows the fitting of MG experimental diffusional profiles to a pure diffusional model. In this case, fitting is deficient and D_{app} depends on the time at which the profile is taken. Here, the best fit is with a model considering diffusion coupled with adsorption on the silica surface. As can be appreciated comparing the diffusion coefficients obtained by both models (insets of Fig. 2a and b, respectively), the retardation effect produced by adsorption of the dye on the silica surface is significant, resulting in D_{app} more than one order of magnitude smaller than D_{eff}. On the other hand, when adsorption is explicitly considered, the calculated MG effective diffusion coefficients for all hydrogel samples are constant in time and slightly differ from one hydrogel sample to another (see inset of Fig. 2b). Furthermore, when these D_{eff} are divided by the pore fraction of each sample, the same value, D_{MG} = (1.5 ± 0.1) 10^{-10} m^2 s^{-1}, is obtained.

Although the values of pure diffusion coefficients obtained for XO and MG dyes are of the same order of magnitude, it is important to note that one should expect a lower intrinsic diffusion coefficient for XO than for MG, as the former is a bulkier molecule. As the hydrogels have similar tortuosity, this discrepancy can be explained by considering differences in constrictivity for both molecules. This parameter accounts for the fact that only a fraction of the porosity is used as a pathway for the diffusion of molecules due to geometrical factors (geometrical constrictivity), and for electrostatic interactions with pore walls (electrostatic constrictivity) [40]. Considering that MG is a positively charged dye these interactions lead to a decrease in D_{eff}.

Concerning the adsorption of MG on the silica surface, the fitting parameters P obtained for each of the samples are in good agreement with the partition coefficients derived from empirical MG adsorption isotherms (P_{emp} = ratio of adsorbed molecules to molecules in solution in a given hydrogel volume, for a C_{eq} = 0.01 - μM) and follow the same trend as the calculated specific adsorption areas derived from aerogel porosimetry and pore fraction volumes (Table 1). The raw data of these experiments are presented in Supplementary Information.

Transport properties depend on the porosity and tortuosity of the material, and thus they are related to the material microstructure. In order to establish a structure–property relationship hydrogels were submitted to supercritical drying, giving aerogels for which it is assumed that the porosity and the particle size of the silica backbone are the same than those of the original wet gel. The Microstructural parameters of aerogels obtained from hydrogels synthesized at different pH values are summarized in Table 2. The synthesis pH of LUDOX-silicate gels allows a fine tuning of microstructure, and the porosity of the matrix is a key parameter in determining mass transport phenomena.

Structural differences produced by varying the synthesis pH, such as particle size and average pore diameter of the corresponding aerogels have negligible influence on the diffusion of soluble species through the water filled hydrogel pores as the pore radii are well above the size of the solvated diffusing dyes. However, the fine tuning of transport properties is given by the adsorption

Table 2
Microstructural parameters of aerogels obtained from hydrogels synthesized at different pH.

Sample	Pore diamete/nm[a]	$a_{s,BET}$/m^2 g^{-1}[b]	Elemental particle/nm[c]	Primary cluster/nm[c]	Secondary cluster/nm[c]
AG-4.5	6.4; 8.1	355 ± 18	7.6 ± 1.9; 13.8 ± 2.6	42 ± 7	133 ± 19
AG-7.0	8.4; 10.6	296 ± 15	16.2 ± 3.4	52 ± 5	164 ± 26
AG-9.0	8.7; 10.5	263 ± 13	16.4 ± 3.2	56 ± 6	210 ± 32

[a] From aerogel porosimetry (BJH Adsorption average pore diameter; BJH Desorption average pore diameter).
[b] From aerogel porosimetry (BET surface area).
[c] As derived from FESEM images of aerogels.

retardation effect, since at pH > 3 the silica surface increases its negative charge that induces adsorption of positively charged species, and in consequence an additional energetic barrier for mass transport. This is the main effect to be considered in transport processes where the synthesis pH accounts for different surface area and pore volume fraction.

In previous works on the silicate-LUDOX route to design cell encapsulation host, [17] a simpler model was applied to characterize the solute transport in hydrogels, obtaining apparent diffusion coefficients, D_{app}, which are valid in restricted conditions. Although these apparent diffusion coefficients allow to compare mass transport on different samples under the same conditions, the calculated D_{app} depends on distance and time, thus on the dye concentration. This dependence on dye concentration in turn determines the fraction of dye free to diffuse and adsorbed on the silica surface.

3. Conclusions

The method proposed herein allows evaluating the effect of the texture of the silica material as well as the charge of the diffusing molecule in the transport process. The simplicity of acquisition of the experimental data (by means of a desk scanner) and further mathematical modeling is in line with high throughput screening procedures, enabling rapid and simultaneous determination of relevant diffusion and adsorption parameters. This will contribute to a rapid screening of the best suited materials for a rational design of silica encapsulation applications.

In particular, the method contributes to the design of materials with biological activity where the fine tuning of mass transport can be achieved by changing the surface charge of the silica skeleton, either by modifying the working pH – which is not always possible for biological systems – or by derivatizing the silica surface with appropriate biocompatible molecules.

Acknowledgments

This work has been supported by National Research Council of Argentina (CONICET PIP 11220110101020), the University of Buenos Aires (UBACyT 20020100100636), National Agency for Science and Technology Promotion of Argentina (PICT-2012-1167) and Brazilian Syncrotron Light Laboratory (SAXS1-13426 and SAXS1-15361). SAB, MJ and MP are Research Scientists of CONICET (Argentina). The authors thank Dr. Thibaud Coradin for fruitful scientific discussions.

Appendix A. Supplementary material

Supplementary data associated with this article can be found, in the online version, at http://dx.doi.org/10.1016/j.jcis.2014.03.030.

References

[1] C.J. Brinker, G.W. Scherer, Sol–Gel Science: The Physics and Chemistry of Sol–Gel Processing, Academic Press, 1990.
[2] C. Sanchez, P. Belleville, M. Popall, L. Nicole, Soc. Rev. 40 (2011) 696–753.
[3] G.J.A.A. Soler-Illia, P. Innocenzi, Chem. -A Eur. J. 12 (2006) 4478–4494.
[4] E.H. Otal, P.C. Angelomé, S.A. Bilmes, G.J.A.A. Soler-Illia, *Adv. Mat.* 18 (2006) 934–938.
[5] A. Léonard, P. Dandoy, E. Danloy, G. Leroux, C.F. Meunier, J.C. Rooke, B.-L. Su, Chem. Soc. Rev. 40 (2011) 860–885.
[6] M. Blondeau, T. Coradin, J. Mater. Chem. 22 (42) (2012) 22335–22343.
[7] N. Nassif, J. Livage, Chem. Soc. Rev. 40 (2) (2011) 849–859;
C. Depagne, C. Roux, T. Coradin, Anal. Bioanal. Chem. 400 (2011) 965–976.
[8] G.S. Alvarez, M.F. Desimone, L.E. Diaz, Appl. Microbiol. Biotechnol. 73 (2007) 1059–1064.
[9] M. Perullini, M. Jobbágy, M. Bermúdez Moretti, S. Correa García, S.A. Bilmes, Chem. Mater. 20 (2008) 3015–3021.
[10] N. Nassif, O. Bouvet, M.N. Rager, C. Roux, T. Coradin, J. Livage, Nat. Mater. 1 (1) (2002) 42–44.
[11] M.L. Ferrer, Z.Y. Garcia-Carvajal, L. Yuste, F. Rojo, F. Del Monte, Chem. Mater. 18 (6) (2006) 1458–1463.
[12] M. Perullini, Y. Ferro, C. Durrieu, M. Jobbágy, S.A. Bilmes, Sol–gel silica platforms for microalgae-based optical biosensors, J. Biotechnol. (2014), http://dx.doi.org/10.1016/j.jbiotec.2014.02.007.
[13] M. Perullini, M. Jobbágy, G.J.A.A. Soller-Illia, S.A. Bilmes, Chem. Mater. 17 (2005) 3806–3808.
[14] M. Perullini, M. Rivero, M. Jobbágy, A. Mentaberry, S.A. Bilmes, J. Biotechnol. 127 (2007) 542–548.
[15] S. Boninsegna, P. Bosetti, G. Carturan, G. Dellagiacoma, R. Dal Monte, M. Rossi, J. *Biotechnol.* 100 (2003) 277–286.
[16] D. Rodrigues, T.A.P. Rocha-Santos, A.C. Freitas, A.M.P. Gomes, A.C. Duarte, Sci. Total Environ. 461–462 (2013) 126–138.
[17] M. Perullini, M. Jobbágy, N. Mouso, F. Forchiassin, S.A. Bilmes, *J. Mater. Chem.* 20 (2010) 6479–6483.
[18] B. Amsden, Macromolecules 31 (1998) 8382–8395.
[19] D.M. Ruthven, Chem. Eng. Sci. 59 (2004) 4531–4545.
[20] D.M. Ruthven, L. Heinke, J. Kärger, Microporous Mesoporous Mater. 132 (2010) 94–102.
[21] D.M. Ruthven, Principles of Adsorption and Adsorption Processes, John Wiley & Sons, New York, 1984.
[22] F. Alexander, V.J.P. Poots, G. McKay, Ing. Eng. Chem. Process Des. Dev. (1978) 406–410.
[23] F. Ye, M.M. Collinson, D.A. Higgins, *Phys. Chem. Chem. Phys.* 11 (2009) 66–82.
[24] B.A. Westrin, A. Axelssonb, G. Zacch, J. Controlled Release 30 (1994) 189–199.
[25] J. Jianhong Pei, M.L. Tercier-Waeber, J. Buffle, G.C. Fiaccabrino, M. Koudelka-Hep, Anal. Chem. 73 (2001) 2273–2281.
[26] G. McKay, Chem. Eng. Sci. 39 (1984) 129–138.
[27] J.V. Brakel, P.M. Heertjes, Int. J. Heat Mass Transfer 17 (1974) 1093–1103.
[28] D.E. Liu, C. Kotsmar, F. Nguyen, T. Sells, N.O. Taylor, J.M. Prausnitz, C.J. Radke, Ind. Eng. Chem. Res. 52 (50) (2013) 18109–18120.
[29] K. Nakanishi, S. Adachi, S. Yamamoto, R. Matsuno, A. Tanaka, T. Kamikubo, Agric. Biol. Chem. 41 (12) (1977) 2455–2462.
[30] Y. Fukushima, K. Okamura, K. Imai, H. Motai, Biotechnol. Bioeng. 32 (5) (1988) 584–594.
[31] D.J. Dickson, B. Lassetter, B. Glassy, C.J. Page, A.F.T. Yokochi, R.L. Ely, Colloids Surf. B 102 (2013) 611–619.
[32] N. Tantemsapya, J.N. Meegoda, Environ. Sci. Technol. 38 (2004) 3950–3957.
[33] E. Ray, P. Bunton, J.A. Pojman, *Am. J. Phys.* 75 (2007) 903–906.
[34] M. Perullini, M. Amoura, C. Roux, T. Coradin, J. Livage, M.L. Japas, M. Jobbagy, S.A. Bilmes, *J. Mater. Chem.* 21 (2011) 4546–4552.
[35] <http://rsb.info.nih.gov/ij/download.html>.
[36] R.L. Burden, J.D. Faires, Numerical Analysis, 3rd Ed., Prindle, Weber and Schmidt, Boston, 1985.
[37] S. Lowell, J.E. Shields, M.A. Thomas, M. Thommes, Characterization of Porous Materials and Powders: Surface Area, Pore Size and Density, Kluwer Academic Publishers, 2004.
[38] J.R. Wujek, D.R. Hafemann, Exp. Neurol. 53 (1976) 166–167.
[39] R. Takahashi, S. Sato, T. Sodesawa, H. Nishida, Phys. Chem. Chem. Phys. 4 (2002) 3800–3805.
[40] D. Jougnot, A. Revil, P. Leroy, Geochim. et Cosmochim. Acta 73 (2009) 2712–2726.